



Crustal structure of the Central Precordillera of San Juan, Argentina (31°S) using teleseismic receiver functions



Jean-Baptiste Ammirati^{a,b,*}, Patricia Alvarado^{a,c}, Marcelo Perarnau^{a,c}, Mauro Saez^a, Guillermo Monsalvo^{a,b}

^a *Departamento de Geofísica y Astronomía, Facultad de Ciencias Exactas, Físicas y Naturales (FCEFYN) de la Universidad Nacional de San Juan, Meglioli 1160 Sur, 5406 Rivadavia, San Juan, Argentina*

^b *Agencia Nacional de Promoción Científica y Tecnológica (ANPCyT-FONCYT), Argentina*

^c *Consejo Nacional de Investigaciones Científicas y Técnicas (CONICET), Argentina*

ARTICLE INFO

Article history:

Received 28 November 2012

Accepted 26 May 2013

Keywords:

Andean retroarc

Flat slab

Décollement

Partial eclogitisation

Continental crust

Moho

ABSTRACT

The subduction of the Nazca plate under the South American plate around 31°S is characterized by flat slab geometry. The (Chilean) Pampean flat slab of Argentina associated with the subduction of the Juan Fernandez ridge lies in a region of a series of foreland uplifts corresponding to the thin-skinned Precordillera and basement cored Sierras Pampeanas ranges. The SIEMBRA project deployed 40 broadband stations in 2008–2009 in both the Precordillera and the Sierras Pampeanas with the aim to foster the understanding of the entire central Andean flat slab region. One of the SIEMBRA station (DOCA) located on the western flank of Sierra de la Invernada in the Central Precordillera appears particularly appropriate to study the crustal structure and eventually detect discontinuities related to terranes establishment. We thus performed a receiver function analysis using teleseismic data recorded at the DOCA station during the SIEMBRA project and from October 2011 to June 2012 using a broadband UNSJ (National University of San Juan) seismic station with the purpose to obtain crustal images with details of the intracrustal structure consistent with a mechanism that could explain both the observed earthquake depths and the uplift pattern in the Central Precordillera. Our results show that the Moho beneath the Precordillera lies at a depth of about 66 km. The Moho signal appears diminished and behaves irregularly as a function of azimuthal orientations. Although this observation could be the result of an irregular geometry it also correlates with the hypothesis of partial eclogitisation in the lower crust. Two mid-crustal discontinuities have also been revealed. The shallower one could correspond to a décollement level between the Precordilleran strata and the Cuyania basement at 21 km depth. The deeper one which the presence has been matched with a sharp decrease of the crustal seismic activity drove us to the hypothesis of a major change in crustal composition at 36 km. Finally the flat portion of the subducted slab has been imaged lying at about 100 km depth.

© 2013 Elsevier Ltd. All rights reserved.

1. Introduction

The subduction of the Nazca plate beneath the South American plate led to the formation of the longest active orogenic system visible on the Earth surface. The Andean cordillera has developed along more than 8000 km of the Pacific active margin of South America, from the Caribbean Sea in the north to the transition with the Magallanes–Fagnano transform margin of Tierra del Fuego Island

in the south. It also includes the highest continental peak of America (Cerro Aconcagua: 6960.8 m above sea level, [UNCUYO, 2012](#)).

One of the outstanding features of the Andes lithosphere is the along-strike variation in the dip angle of the subducting plate (subhorizontal and ~30° to the east). At least two segments of flat slab geometry have been evidenced using seismic locations corresponding to the Peruvian (3°S–18°S) and the Chilean (27°S–33°S) flat slab regions ([Cahill and Isacks, 1992](#)). Both regions shared similar features such as the absence of active volcanism in the main cordillera and the presence of a subducting aseismic ridge (respectively the Nazca ridge and the Juan Fernandez ridge) highly suspected to be one of the key-factors in the slab flattening process ([Pilger and Handshumacher, 1981](#); [Yáñez et al., 2002](#)).

* Corresponding author. Departamento de Geofísica y Astronomía, Facultad de Ciencias Exactas, Físicas y Naturales, Universidad Nacional de San Juan, Meglioli 1160 Sur, Rivadavia 5406, San Juan, Argentina. Tel.: +54 264 4234129x203.

E-mail address: jb.ammirati@unsj-cuim.edu.ar (J.-B. Ammirati).

In the South Central Andes, Cenozoic tectonic shortening has recorded a series of thin-skinned and thick-skinned foreland uplifts (the Argentine Precordillera and the Sierras Pampeanas, respectively) above the Chilean-Pampean flat slab region around 31°S, probably induced by the flat subduction processes (Isacks et al., 1982; Jordan et al., 1983; Jordan and Allmendinger, 1986; Ramos and Kay, 1991, 2002; Kay and Abbruzzi, 1996). More recently, neotectonic studies, GPS surveys and real time seismic monitoring indicate that the uplift of the Precordillera as well as the Sierras Pampeanas is based on reactivation of previous normal faulting which were inverted during Neogene and still continue (Uliana et al., 1995; Ramos et al., 2002; Brooks et al., 2003). In addition, the Precordilleran crust may have formed as a result of different accreted terranes onto the Gondwana western margin at Ordovician times. Thus, the site of the seismic station DOCA at about 31°S (Fig. 1) can help to detect changes in crustal structure related to differences in terrane provenance.

Receiver function (RF) analysis is a powerful technique to model the crustal and mantle earth structure. It considers waveforms from distant earthquakes that are traveling through the earth and will generate reverberations (basically, P-wave to S-wave conversions) when crossing discontinuities in seismic velocities. The difference in travel times between the direct and converted phases, as well as their amplitudes, recorded at a three-component seismological station contains information about the structure responsible for the reverberations beneath the recording station. Using earthquakes as a seismic source makes the receiver function analysis particularly adapted for deep structure imaging. In this study, exploration of the crustal structure around the seismic station DOCA is carried out using teleseismic receiver functions analysis, which is interpreted on a base of seismological and geological studies in this region.

2. Previous seismic regional studies

Many investigators successfully used receiver function analysis across the world and particularly in the Pampean flat slab region of the south central Andes in order to image upper mantle and crustal discontinuities as well as relationships between shallow faulting

and deeper structures. Thus, using local receiver functions, Calkins et al. (2006) observed a Moho signal at a depth of approximately 50 km and two mid-crustal arrivals at 20 and 34 km beneath San Juan in the southwest of Sierra de Pie de Palo (western Sierras Pampeanas). Their results are consistent with previous observations in the same region using different methods by Comínguez and Ramos (1991), Zapata (1998), Fromm et al. (2004) and McGlashan et al. (2008). Perarnau et al. (2010) put more constraints using a longer record of receiver functions from higher magnitude teleseismic events defining a Moho signal at approximately 47 km, and two mid-crustal signals at 13 and 28 km. In view of the location of these results for the San Juan area lying in the transition zone between the western Sierras Pampeanas and the eastern Precordillera, the intra-crustal discontinuities were interpreted as décollements within the Cuyania terrane. Gans et al. (2011) used data from the two-year SIEMBRA experiment, combining teleseismic receiver function traces with the common conversion point (CCP) stacking method and proposed 2D cross-sections at different latitudes for the entire flat slab region. Although Gans et al.'s studies were focused on the morphology of the flat slab, they were able to show the Moho at a depth close to 50 km under the Sierras Pampeanas, ~60 km under the Precordillera more to the west and 70–80 km under the Frontal and Principal Andean Cordillera. These values are coherent with previous results from Introcaso et al. (1992) and Gilbert et al. (2006).

The flat slab has been imaged using receiver functions by Gans et al. (2011) lying at 100 km beneath San Juan which is consistent with the seismic locations (Anderson et al., 2007). However, like Gilbert et al. (2006), difficulties were experienced mapping the Moho with the same precision beneath the Central Precordillera. According to their interpretation, the lack of a sharp Moho signal at this specific area could be caused by a diminished contrast between lower crust and upper mantle properties due to partial eclogitisation of the lower crust. Using depth phase precursors analysis, McGlashan et al. (2008) also inferred the presence of a crustal mafic root beneath the Western Precordillera. In addition, this zone is also supposed to be structurally complex due to crustal shortening

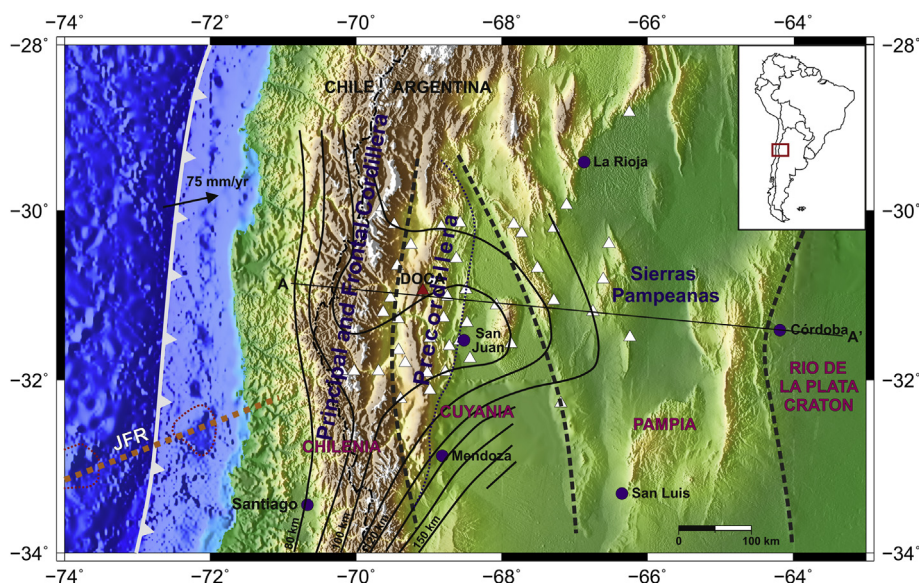


Fig. 1. Location map showing major features relative to the Pampean flat slab region of Argentina. The solid black lines represent contours of the top of the subducted Nazca plate from Cahill and Isacks (1992), redefined by Anderson et al. (2007). White triangles mark locations of the SIEMBRA project broadband seismic stations. The red triangle localizes the broadband seismic station DOCA (Don Carmelo). Dark grey dashed lines show main suture zones between the different terrane. The Juan Fernández Ridge (JFR) is materialized by the orange dashed line (Global direction) and red dashed circles (subducting seamounts). The convergence between the Nazca plate and the south-American plate is represented by the black arrow (DeMets et al., 2010). The straight black solid line outlines the cross section (AA') presented in Fig. 7a. (For interpretation of the references to color in this figure legend, the reader is referred to the web version of this article.)

induced by the flat subduction (Ramos et al., 2002; Gilbert et al., 2006; McGlashan et al., 2008; Alvarado et al., 2009).

In this study we computed teleseismic receiver functions for a seismological station (DOCA) located at 30.95°S and 69.08°W in the western flank of the Sierra de la Invernada, Central Cordillera, in order to get more detailed images of the structure of the crust, its thickness and possible variation in morphology. The results are analyzed in view of other available studies trying to find relationships at levels of deep and shallow crust. Our dataset include information from the permanent station DOCA collected in the SIEMBRA 2008–2009 experiment and later.

3. Data and methods

The Sierras Pampeanas Experiment using a Multicomponent Broadband Array (SIEMBRA) was carried out with the goal to enhance the understanding of the central Andean flat slab region (west central Argentina between 30°S and 32°S). It consisted of 40 broadband stations using a grid spacing of 15–20 km with denser observations preferentially in the predicted flat slab zone (Fig. 1). The SIEMBRA network deployed in 2007–2008 recorded hundreds of teleseismic events and more than 90,000 local events according to Gans et al. (2011).

We computed teleseismic receiver functions for one SIEMBRA seismological station, which is still continuously monitoring using a broadband station from the National University of San Juan. This station is located in the Central Cordillera, more precisely inside the natural reserve Don Carmelo (DOCA) at 30.95°S and 69.08°W. Thus, using approximately two years and a half of seismic data, we selected events with epicentral distances between 25° and 95° and considered their P phases only. We noted that earthquakes with moment magnitude (Mw) greater than 6 were optimal avoiding noisy traces. The selected events were then bandpass filtered from 0.15 to 5 Hz producing a good quality signal with no contamination of anthropogenic noise or microseismic events. The next step consisted of visually inspecting one by one the filtered waveforms in order to get rid of the remaining poor quality traces (low signal/noise ratio, weak P-wave arrival and bad recorded traces). 37 out of the 80 teleseismic earthquakes between March 2008 and November 2009 (USGS) during the SIEMBRA project passed the inspection with these criteria. 10 more teleseismic events were also added, which were recorded at DOCA between October 2011 and June 2012 and selected following the same process (Fig. 2).

Thereafter, for each event, we synchronized the three components, removed the mean and rotated the observed vertical, north-south and east-west seismograms into vertical, radial and tangential components to receive the information in the direction of the great circle path. In the time domain, the theoretical displacement generated at the earth surface by a P plane wave can be expressed as the convolution of the source term (source time function), the earth impulse response and the instrumental impulse response (Langston, 1979). By deconvolving the radial or tangential component by the vertical component it is possible to get rid of both the source and the instrumental response terms. The resulting waveform is a causal (not anticipative), clean, seismogram-like signal corresponding to the earth impulse response and it is also called (radial or tangential) receiver function (RF). A RF is thus a time-series of Gaussian spikes and each spike corresponds to a P-to-S converted wave arrival that reverberated in the structure beneath the seismometer (Fig. 2b and c). Our RFs were computed using a time domain deconvolution technique (Ligorria and Ammon, 1999) where the RF is iteratively formed and convolved with the vertical component to create a synthetic radial or tangential seismogram. A misfit between real and synthetic amplitudes is then estimated (classical variance reduction). The process lasts until the improvement of the misfit become

insignificant ($\leq 0.01\%$). The width of the Gaussian filter used in the deconvolution acts as a low-pass filter. It can be adjusted to highlight different features of interests. Thus, the higher the Gaussian value, the better the resolution but more noise is included and could destabilize the deconvolution. After testing our data at DOCA station using Gaussian filters of 1, 2.5, 4 and 5 widths (corresponding to lowpass filters of corner frequencies 0.5, 1.2, 2 and 2.4 Hz, respectively), it seemed that a Gaussian width of 2.5 is the best quality/resolution trade-off.

Once the RFs were computed, the traces were visually inspected and those presenting negative first arrivals, long period trends or harmonic oscillations were discarded. Finally, 24 radial receiver functions were retained and used for interpretation (Fig. 2).

4. Results

One simple method to avoid confusions interpreting RF traces consists in plotting a receiver function phasing diagram as a function of ray parameter (which is related to the epicentral distance). This diagram is called moveout plot. The RFs presenting the same ray parameter are binned, averaged and finally plotted as a function of slowness (Gurrola et al., 1994). The moveout plot combined with the theoretical arrivals allows us to discriminate primary arrivals from multiples phases (reverberations) or noise. The primary arrivals versus ray parameter exhibit a positive slope (increasing arrival time with increasing ray parameter) while multiple phases present a negative slope (decreasing arrival time with increasing ray parameter).

The moveout plot performed for the DOCA station (Fig. 3) shows a clear strong positive signal 2-to-3 seconds after the direct P-wave arrival with corresponding reverberated phases, PpPs (positive) and PsPs + PsSs (negative) at respectively ~ 10 and ~ 13 s after the first P-wave arrival. Fig. 3 shows that this direct P-wave arrival presents the wrong moveout (decreasing arrival time with increasing slowness). This is probably due to poor azimuthal distribution. However, traces presenting a low slowness (~ 0.04 s/km) come from far events ($\sim 90^\circ$). Events corresponding to that distance form a group globally localized to the west at the New Zealand subduction zone (Fig. 2a and d). Late arrivals could also be caused by a west-dipping interface of the discontinuity responsible for the observed signal. A slight positive primary arrival is observed 5–6 seconds after the direct P-wave arrival with its multiple phases encountered at approximately 16 and 21 s. This signal is dependent on the ray parameter (stronger signal for higher values of ray parameter). Then, we observe with an 8-s delay, a strong but also slowness-dependent (greater amplitude for lower values of ray parameter) positive signal likely caused by the Mohorovicic discontinuity. The multiples phases of this arrival are clearly shown around 27 s (PpPs) and 36 s (PsPs + PsSs). In addition, 12 s after the first P-wave arrival approximately, it is possible to observe a clear negative signal with a positive moveout. Its corresponding first reverberated phase (negative in this case) is visible 38–39 s after the direct P-wave arrival. This particular case is theoretically observed for a velocity contrast showing a decreasing seismic velocity. This decreasing in velocity is probably related to the presence of the oceanic crust in the subducting slab lying at about 100 km (Pardo et al., 2002; Anderson et al., 2007; Gans et al., 2011).

Considering those results, we constructed a simple three-layer crust over mantle model. For each layer, the P seismic velocity (V_p), P–S seismic velocity ratio (V_p/V_s) and the density (ρ) were initially chosen using *a priori* values coming from previous studies (Gilbert et al., 2006; Alvarado et al., 2007; Wagner et al., 2008; Linkimer et al., 2010; Gans et al., 2011). Based on this preliminary model we computed synthetic receiver functions and performed synthetic moveout plots (Fig. 3). Matching both real and synthetics

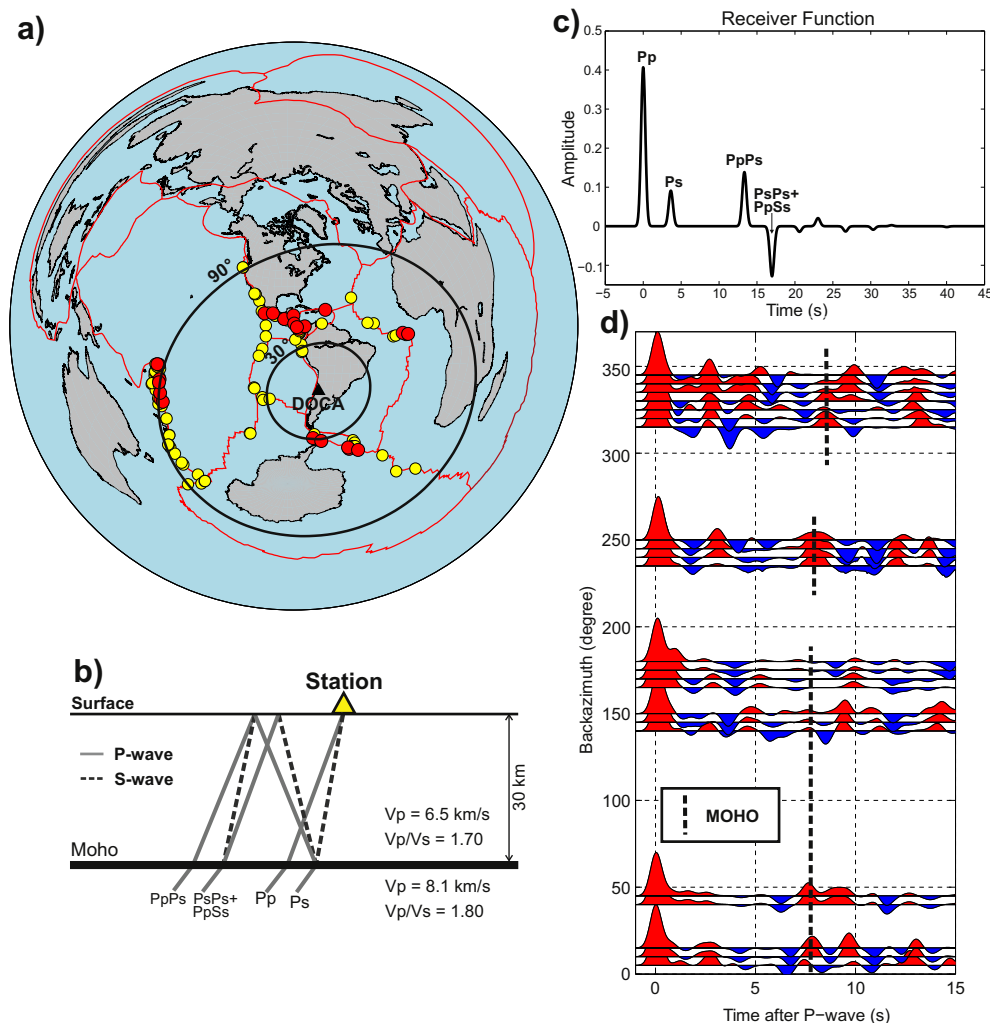


Fig. 2. a) Epicenter distribution of teleseismic earthquakes (Yellow dots) recorded by the Broadband seismological station DOCA during the SIEMBRA project (2008/03/29 to 2009/11/23) and under National University of San Juan monitoring (from 2011/10/07 to 2012/06/22). Earthquakes which provided exploitable receiver functions are red dots. Red solid lines materialize plate boundaries. b) Ray paths for direct P wave (Pp), P to S converted wave (Ps) and reverberated phases (PpPs, PsPs + PpSs) crossing a flat Moho in a single layer over a half space model and recorded in one single seismic station. c) Associated synthetic radial receiver function for the crustal model shown in b). d) Azimuthal variation of the radial component of receiver functions used in this study. Positive amplitudes are in red, negative amplitudes are in blue. Vertical dashed lines mark the position of the Moho signal. (For interpretation of the references to color in this figure legend, the reader is referred to the web version of this article.)

arrivals with theoretical arrivals (solid lines in Fig. 3) we iteratively (trial-and-error) adjusted the V_p , V_p/V_s , geometry of discontinuities (depth and dip) and velocity variations. Testing these parameters directly controls the amplitude of the arrivals between the different layers and allowed us to improve our model in order to get the most accurate estimation (Fig. 4). Direct arrivals (Ps) are not very sensitive to V_p and V_p/V_s variations but this is the case for reverberated phases (PpPs and PsPs + PpSs). That is why reverberated (real and synthetics) arrivals have also been matched with theoretical multiple phases (solid lines in Fig. 3a) to enhance the reliability of the model. The good agreement of our obtained model is shown in Fig. 4b. We used a cross-correlation to estimate the similarity between real and synthetic data. Both real and synthetic traces were corrected from moveout and stacked in one single trace to be compared. Basically for each point in time along RFs, we calculated the travel time and determined the corresponding depth. Resulting traces are then averaged in one single trace. Considering that real data is noisy due to the complexity of the structure beneath DOCA and the depth of the investigated structures, we evaluated the covariance within the first 15 s after the

first P-wave arrivals. Comparing real and synthetics data also helped us to adjust the velocity contrast by matching amplitudes of the different arrivals.

Our best results indicate a model where the first crustal discontinuity is lying at a depth of 21 km exhibiting a high velocity jump (V_p increasing from 5.8 to 6.5 km s^{-1}). The second discontinuity in depth was found at about 36 km depth. It exhibits a much lower amplitude which involves a smoother velocity contrast (6.5–7.0 km s^{-1}) and delimitates two different zones within the lower part of the crust. The Moho signal is particularly difficult to distinguish because it seems to behave irregularly in appearance (slowness-dependant) and really close to the first positive multiple associated with the first mid-crustal arrival (21 km). However, our results indicate a Moho depth beneath the Andean Central Pre-cordillera (31°S) at 66 km. Considering an error of 10% in the maximum amplitude determination for the Moho signal, we estimated the uncertainty of the Moho depth to be of about 2 km. Thus, the obtained depth is coherent with observations and results provided by previous studies carried on the same area and using seismic broadband data (Gilbert et al., 2006; Gans et al., 2011). It is

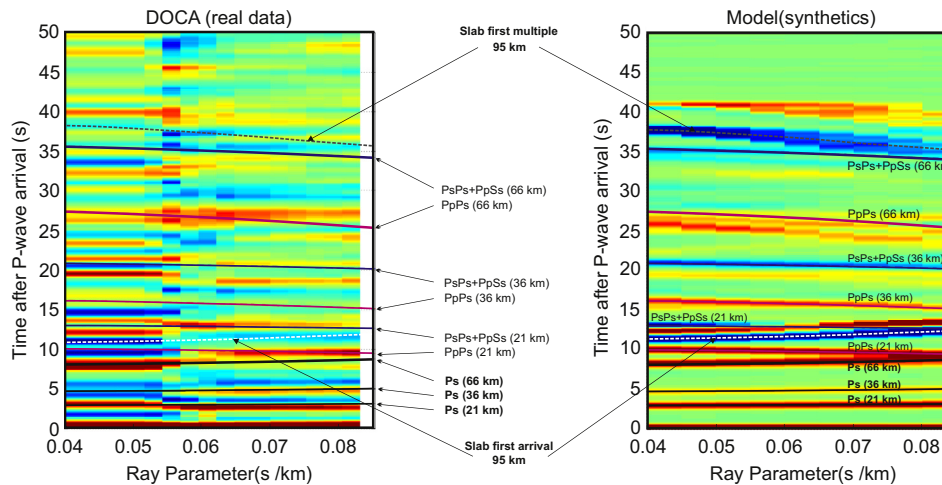


Fig. 3. (left) Radial receiver function versus ray parameter (moveout plot) for the DOCA station (see Fig. 1 for location). (Right) Moveout plot using synthetic radial receiver functions. Positive amplitudes are in red, negative amplitudes are in blue. Solid lines represent the theoretical arrivals for Ps (black), PpPs (pink) and PsPs + PpSs (deep blue). Travel time curves were calculated using the velocity model described in the main text and in Fig. 4a. (For interpretation of the references to color in this figure legend, the reader is referred to the web version of this article.)

interesting to note that our best model indicate a possible inclination for the Moho of about 10–12° to the west. There are no significant differences for values inside this range. Interestingly, the Moho depth beneath the Sierra de Pie de Palo in the Western Sierras Pampeanas was estimated by Calkins et al. (2006), McGlashan et al., 2008 and Perarnau et al. (2010) at about 50 km depth. Several hundred kilometers westward, Gilbert et al. (2006), McGlashan et al., 2008 and Gans et al. (2011) imaged the Moho under the high Andean Cordillera at a depth close to 70 km. Considering those two last adjacent regions, it is possible to see that the mean slope for the Moho between the western Sierras Pampeanas and the Cordillera is of about 8°, dipping to the west which is in good agreement with our estimated model. The geometry of the structures responsible for wave reverberations impacts directly on the characteristics of the associated RFs in terms of timing, amplitude and polarity (Cassidy, 1992; Hayes and Furlong, 2007; Linkimer et al., 2010). A dipping interface may thus generate RFs with strong azimuthal variations. This is why it is important to specifically consider this effect.

5. Discussion

5.1. First mid-crustal arrivals

The shallow deformation observed in the flat slab region of the central Andes at ~31°S, is characterized by two opposed thrust system (Ramos, 1988). At the east, the Sierras Pampeanas and the eastern Precordillera present east dipping main thrust structures whereas the central Precordillera around DOCA station, presents mainly west dipping thrusting (Figuroa and Ferraris, 1989; Von Gosen, 1992). This series of foreland uplift likely induced by regional crustal shortening during late Cenozoic, have been related to the reactivation of deeper and older structures, like sutures and shear zones (e.g: ophiolitic shear zone of Valle Fértil – La Huelta) formed during the Paleozoic complex accretion of different terranes (Ramos et al., 1998, 2002; Vergés et al., 2007). From Cambrian to late Ordovician, the oceanic lithosphere at the eastern margin of the Precordillera terrane subducted under the Gondwana, causing east dipping deformation of its margin (Astini et al., 1995). Using RF

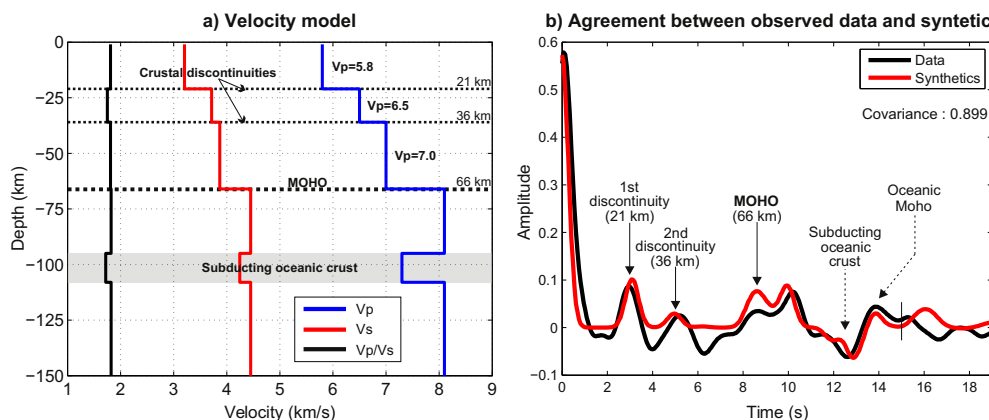


Fig. 4. a) Graphic representation of the obtained velocity model. V_p (blue), V_s (red) and the ratio V_p/V_s (black) are plotted as a function of depth. b) Agreement between observed (black) and synthetic data (red). The curves have been obtained after moveout correction and stack of real and synthetic radial receiver functions respectively. The similarity (covariance) between real and synthetic data has been evaluated using cross-correlation (lag = 0 s) before the vertical tick (15 s after direct P-wave arrival). (For interpretation of the references to color in this figure legend, the reader is referred to the web version of this article.)

analysis, Perarnau et al. (2010) found two mid-crustal discontinuities interpreted as décollement levels within the Cuyania terrane and probably related to this episode. A change in the subduction direction from east to west occurred during late Ordovician involving thus the western boundary of the Precordillera terrane may have caused the west dipping thrust system affecting mostly Silurian and Devonian deep marine flysch deposits (González Bonorino, 1973). The mid-crustal discontinuity identified in this study with receiver function at 21 km depth could be part of this important system between the upper sedimentary cover and the Cuyania basement. Crustal structure at the junction between the western Sierras Pampeanas and the eastern Precordillera have been intensely studied (Jordan and Allmendinger, 1986; Cominguez and Ramos, 1991; Ramos et al., 2002; Vergés et al., 2007) and several models, based on geological observations and seismological data, have been proposed. Most of them involve opposing thrust ramps detaching at different crustal levels (Smalley et al., 1993; Allmendinger and Zapata, 1996; Ramos et al., 2002). The central sector of the Precordillera remains however, relatively unknown. Ramos et al. (2002) proposed a structural model where the west dipping faults in the central Precordillera are merging at depth as far as they go to the west and form a décollement level between the upper sedimentary cover and the Cuyania basement. This interpretation is compatible with our observation of a mid-crustal discontinuity lying at 21 km depth. As mentioned in the previous part, this discontinuity likely presents a west dipping interface. Using both the same data and protocols as for DOCA station we computed teleseismic receiver functions for the seismological station (GUAL also part of the project SIEMBRA) in order to gain more information to better understand the overall geometry. This station is located in the Pampa de Gualilán (30.83°S; 68.95°W), ~18 km northeast of station DOCA. The two stations are thus closely located in the Central Precordillera and it is reasonable to assume that the underlying crustal physical characteristics (V_p , V_s , density) are similar. After moveout corrections and time-to-depth conversions

(Fig. 5), the first mid-crustal arrival beneath station GUAL is observed at 18 km depth, which is shallower than the estimated 21 km depth beneath station DOCA in the west. Keeping in mind the effect that the alignment of the stations is not orthogonal to the structures, the apparent slope estimation indicates at least 8° to the west (Fig. 5b). This observation supports the idea of a décollement level at this depth probably corresponding to an old subduction zone active during late Ordovician (González Bonorino, 1973) and responsible for mainly west-dipping structures.

5.2. Second mid-crustal arrivals

According to Ramos (2004) and Sato et al. (2004), the Cuyania terrane seems to extend from north (~27°S) to south (~40°S) including Cambrian to Carboniferous sedimentary cover (particularly visible in the Precordillera) and basement rocks (Chernicoff et al., 2008). Late Meso-Proterozoic metamorphosed basement is visible in Sierra de Pie de Palo in San Juan, Argentina. Some small outcrops of Ordovician strata and basement rocks are also visible close to the town of San Rafael in Mendoza, Argentina, at about 36°S (Ramos, 1995, 2009; Ramos et al., 1998). The origin and the composition of the Cuyania terrane remain highly discussed topics (Bond et al., 1984; Ramos et al., 1986; Dalziel et al., 1996; Finney, 2007) and the presence of deep discontinuities within its basement is not obvious to construe considering the lack of geological evidence concerning the composition of this composite terrane itself. A variation in lithology within the terrane or another décollement level related to terrane establishment able to generate a strong velocity contrast and consequently an identifiable seismic signal is purely hypothetical. However, earthquake tomographic locations by Linkimer (2011) using the SIEMBRA seismological data (Fig. 6) show a sharp seismicity decrease at 35–40 km depth. This observation is consistent with our results highlighting an intracrustal arrival close to 36 km depth; thus, this can be related to a probable change in the physicochemical properties of the crust

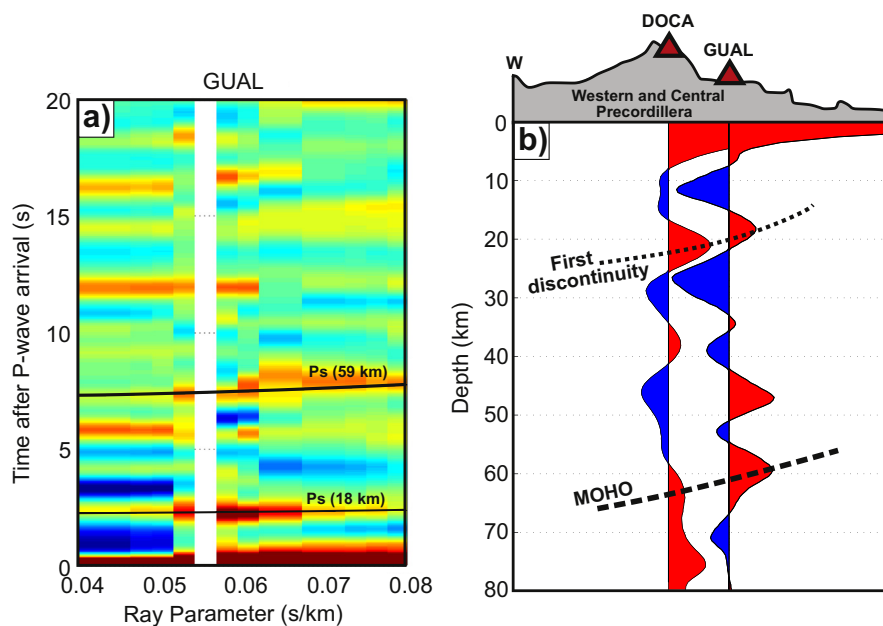


Fig. 5. a) Moveout plot for the station GUAL. Positive amplitudes are in red, negative amplitudes are in blue. Black solid lines are theoretical Ps arrivals for discontinuities lying at respectively 18 and 59 km depths. Theoretical travel times were calculated using the same velocity model as for DOCA. b) E–W transect showing time-to-depth converted receiver function stacks for station DOCA and GUAL. The comparison of the two stacks obtained for stations DOCA and GUAL shows the apparent west dipping of the first mid-crustal discontinuity (21 km). However, note that the stations are not aligned perpendicularly to the regional structures and thus do not permit to put more constrain about the geometry of this intracrustal discontinuity. (For interpretation of the references to color in this figure legend, the reader is referred to the web version of this article.)

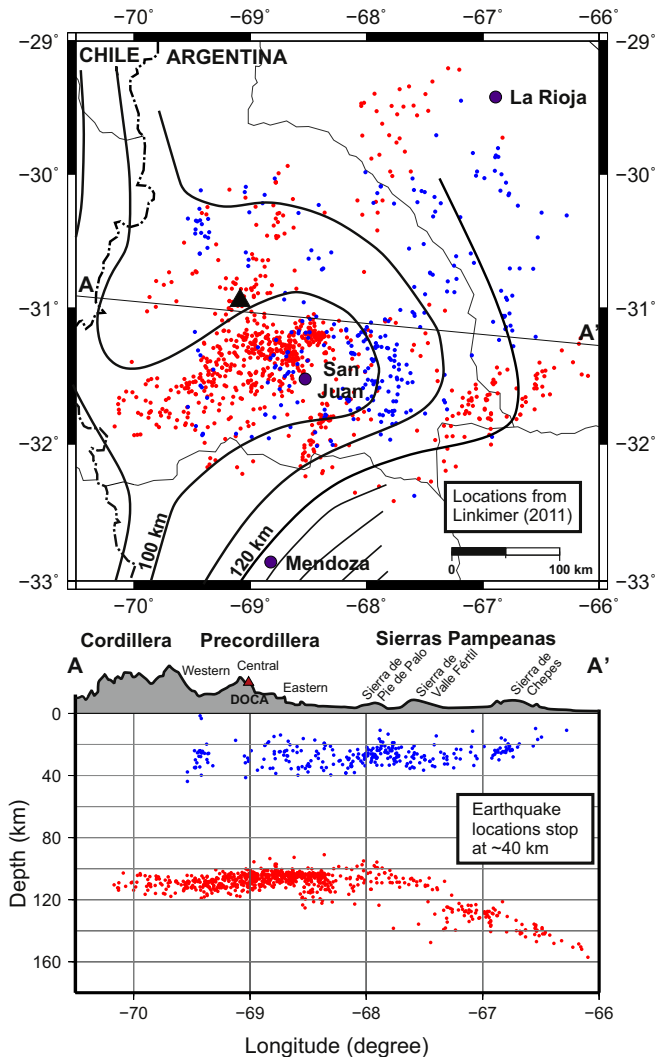


Fig. 6. (top) Epicentral distribution of local earthquakes occurred during the SIEMBRA project (2008–2009). Localizations are from Linkimer (2011). Solid dark grey lines are provincial (Argentina) and regional (Chile) boundaries. The contours of the top of the subducted slab (Anderson et al., 2007) are solid black lines. Blue dots represent crustal event whereas red dots represent intra-slab events. (bottom) Cross section AA' showing the distribution of the seismicity in depth. Note the sharp decrease of crustal seismicity at ~40 Km. (For interpretation of the references to color in this figure legend, the reader is referred to the web version of this article.)

inducing a brittle-ductile transition of the crustal mechanical behavior.

It is worth to note that a classic continental crust is composed of about 60% of SiO₂ (Clarke and Washington, 1924; Pakiser and Robinson, 1966; Taylor and McLennan, 1981; Weaver and Tarney, 1984; Christensen and Mooney, 1995). Quartz begins to behave plastically for temperatures extending from 250 °C to 400 °C depending on the crustal lithostatic pressure. In these conditions, the brittle-ductile limit is generally expected at 15–20 km depth (Scholz, 1990). In our case we observe that the crustal seismicity stops at ~40 km depth which can be considered as an abnormally deep brittle-ductile transition. This suggests that in the region of the study, the entire crust could be enriched with mafic materials keeping the crust brittle up to 35–40 km depths. The density, Vp and Vp/Vs ratio obtained for the crust between 21 and 36 km (Figs. 4 and 7) are compatible with this composition according to Ludwig et al. (1970) and Brocher (2005) laboratory studies. The temperature plays an important role in

crustal rheology, a negative temperature anomaly caused by the presence of the flat slab also might lower the depth of the brittle-ductile transition although there is currently no study confirming this hypothesis. The modeled crustal velocities of 7 km/s between 36 and 65 km depth is coherent with the hypothesis of a partial eclogitisation of the lower crust as suggested by Gilbert et al. (2006) and tested by isostatic models (Alvarado et al., 2009). However, partial eclogitisation probably begins deeper than 36 km. Eclogites are high-pressure, medium-to-high temperature metamorphic rocks and it would be uncommon to observe their presence at this depth except at very high water content (Jin et al., 2001).

5.3. Moho and deeper arrivals

As previously discussed, the wide signal identified ~8 s after the direct P-wave arrival is probably generated by the presence of the Moho, which can be successfully modeled using a strong positive velocity contrast of 7–8.1 km/s and a crustal thickness of 66 km corresponding to the limit between the lower crust and the upper mantle. The unambiguous observation we can make is the variability in the character of the signal in terms of slowness dependence. Thus the slowness for the 24 RFs ranges from 0.0412 to 0.0827 s/km. For values of the ray parameter lower than 0.06 s/km, the signal is clear and strong but for greater values, it exhibits lower amplitudes. In order to accurately fit the data, we have modeled this change in the Moho character assuming a westward inclination of the Moho of about 10–12° which could be one of the reason for a diminished arrival amplitude toward the updip direction (Linkimer et al., 2010). Fig. 2d shows the variation of the Moho signal amplitude as a function of the backazimuth. For the RFs of waveforms globally coming from the southeast (updip direction) the Moho signals show small amplitude and are even nonexistent for backazimuth close to 170°. However, the probable inclination of the Moho beneath the Precordillera is probably not the only one explanation for the observed signal behavior.

As discussed in the previous section, a closer mineralogical composition between the lower crust and the upper mantle resulting from a partial eclogitisation of the lower crust can also be another explanation of a weak and variable Moho signal character. The agreement between real and synthetic data (Fig. 4b) is particularly poor concerning to the amplitude of the Moho signal. The synthetic receiver functions present a much stronger signal than the real data which imply a lower velocity contrast than that one used in our model. The fact that the modeled second mid-crustal arrival fit well the observed data does not match the same interpretation for the Moho signals. Taking together these results suggest an evolution in the physicochemical properties of the lower crust between 36 and 66 km depths. The partial eclogitisation of the lower crust might be gradual involving a higher degree of eclogitisation with a higher volume of mafic material and thus a higher density and wave velocity closer to the Moho depth (Fig. 7b). A similar observation has been done by Calkins et al. (2006) when they investigated the crustal structure beneath the city of San Juan (Western Sierras Pampeanas) at about 50 km depth.

Although the goal of this work was to image details of the precordilleran crust, we have also been able to identify the oceanic crust in the subducting slab beneath station DOCA. According to our results, the subducted oceanic crust has been modeled as lying at 95 km depth, with a thickness of 13 km, a Vp of 7.3 km/s and a Vp/Vs ratio of 1.72. These values are in good agreement with previous receiver function regional studies performed in flat slab region of Argentina by Gilbert et al. (2006) and Gans et al. (2011).

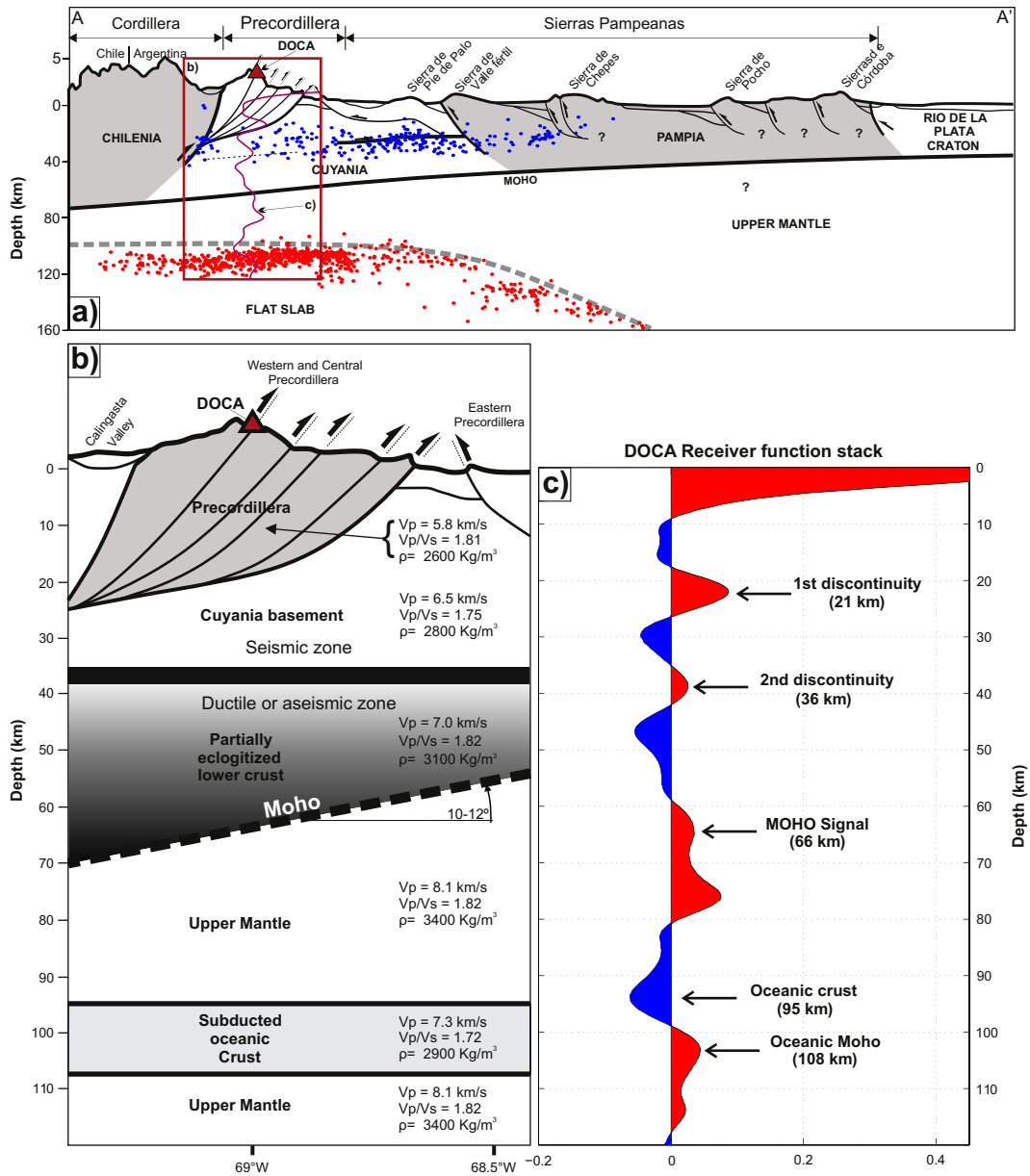


Fig. 7. a) Lithospheric cross-section (AA') of the Pampean flat slab region of Argentina (31°S). The structural interpretation of the eastern Precordillera comes from Ramos et al. (2002). Structures beneath western and eastern Sierras Pampeanas come from Perarnau et al. (2010, 2012). Blue and red dots are seismic locations from Linkimer (2011) also presented in Fig. 6. The red box indicates the study area. b) schematic structural and geophysical crustal model obtained in this study. c) time-to-depth converted receiver function stack for station DOCA. (For interpretation of the references to color in this figure legend, the reader is referred to the web version of this article.)

6. Conclusions

In this study, we investigated the continental crust structure using an iterative pulse-stripping time domain deconvolution technique to compute teleseismic RFs beneath a seismological station located in Central Precordillera, which overrides the Pampean flat slab in central-west Argentina. We found a crustal thickness beneath the Central Precordillera of approximately 66 km. In addition, two mid-crustal discontinuities were also identified at depths of 21 and 36 km, respectively. Based on existing structural studies, the first observed discontinuity (21 km) could be related to the presence of a décollement level between the thin-skinned deformed Precordillera and the Cuyania basement. The identification of a deeper mid-crustal discontinuity at 36 km is coherent with seismological data showing a sharp seismicity decrease between 35

and 40 km depth. This observation suggests a modification at this depth of the lower crust rheology. The abnormally high P-wave velocity modeled between 36 and 66 km as well as the low amplitude observed Moho signal strengthen the hypothesis of a partial eclogitisation of the lower crust. The degree of eclogitisation is likely gradual and increasing with depth. The upper part of the flat slab corresponding to the subducting oceanic crust, have also been imaged lying between depths of 95 and 108 km in good agreement with previous studies. All results and observations are summarized in Fig. 7.

Acknowledgments

We are grateful to the IRIS (Incorporated Research Institutions for Seismology) and its BREQ_FAST interface for easy download of

the teleseismic data used in this study. This research has been supported by the Agencia Nacional de Promoción Científica y Tecnológica (ANPCyT-FONCyT, grant PICTO-Riesgo Sísmico 2007-00233). We would like to thank Arturo Curátola, owner of the Don Carmelo natural reserve for permitting the implantation and the exploitation of the broadband seismological station DOCA. Thanks to Lepolt Linkimer for his participation in the realization of this work especially for providing us data presented in Fig. 6. Thanks to Sofía Pérez and her helpful knowledge in petrology. We are also grateful to Susan Kay and another anonymous reviewer. Their comments were very helpful to improve the quality of this manuscript. Maps were created using the Generic Mapping Tools software (GMT). The project SIEMBRA was supported by the National Science Foundation (EAR-0510966).

References

- Allmendinger, R.W., Zapata, T.R., 1996. Imaging the Andean structure of the Eastern Cordillera on reprocessed YPF seismic reflection data. In: XIII Congreso Geológico Argentino y III Congreso de Exploración de Hidrocarburos. Universidad de Buenos Aires, Buenos Aires.
- Alvarado, P., Beck, S., Zandt, G., 2007. Crustal structure of the south-central Andes Cordillera and backarc region from regional waveform modeling. *Geophysical Journal International* 170, 858–875.
- Alvarado, P., Pardo, M., Gilbert, H., Miranda, S., Anderson, M., Saez, M., Beck, S., 2009. Flat-slab subduction and crustal models for the seismically active Sierras pampeanas region of Argentina, in Backbone of the Americas: shallow Subduction, Plateau Uplift, and Ridge and Terrane Collision. Geological Society of America Memoirs 204, 261–278.
- Anderson, M., Alvarado, P., Zandt, P., Beck, S., 2007. Geometry and brittle deformation of the subducting Nazca Plate, Central Chile and Argentina. *Geophysical Journal International* 171, 419–434.
- Astini, R.A., Benedetto, J.L., Vaccari, N.E., 1995. The early Paleozoic evolution of the Argentine Precordillera as a Laurentian rifted, drifted and collided terrane: a geodynamic model. *Geological Society of America Bulletin* 107, 253–273.
- Bond, G.C., Nickeson, P.A., Kominz, M.A., 1984. Breakup of a super-continent between 625 Ma and 555 Ma: new evidence and implications for continental histories. *Earth and Planetary Science Letters* 70, 325–345.
- Brocher, T.M., 2005. Empirical relations between elastic wavespeeds and density in the Earth's crust. *Bulletin of the Seismological Society of America* 95, 2081–2092.
- Brooks, B., Bevis, M., Smalley, R., Kendrick, E., Manceda, R., Lauría, E., Maturana, R., Araujo, M., 2003. Crustal motion in the Southern Andes (26°–36°S): do the Andes behave like a microplate? *Geochemistry Geophysics Geosystems* 4, 1–14.
- Cahill, T., Isacks, B.L., 1992. Seismicity and the shape of the subducted Nazca plate. *Journal of Geophysical Research* 97, 17503–17529.
- Calkins, J., Zandt, G., Gilbert, H., Beck, S., 2006. Crustal images from San Juan, Argentina, obtained using high frequency local event receiver functions. *Geophysical Research Letters* 33, 1–4.
- Cassidy, J.F., 1992. Numerical experiment in broadband receiver function analysis. *Bulletin of the Seismological Society of America* 82, 1453–1474.
- Chernicoff, C.J., Zappettini, E.O., Santos, J.O.S., Beyer, E., McNaughton, N.J., 2008. Forland basin deposits associated with Cuyania accretion in La Pampa province, Argentina. *Gondwana Research* 13, 189–203.
- Christensen, N.I., Mooney, W.D., 1995. Seismic velocity structure and composition of the continental crust: a global view. *Journal of Geophysical Research* 100, 9761–9788.
- Clarke, F.W., Washington, H.S., 1924. The composition of the Earth's crust. *Geological Survey Professional Paper* 127, 1–117.
- Comínguez, A.H., Ramos, V.A., 1991. La Estructura Profunda entre Precordillera y Sierras Pampeanas de la Argentina, Evidencias de la Sísmica de Reflexión Profunda. *Revista Geológica de Chile* 18, 3–14.
- Dalziel, I.W.D., Dalla Salda, L., Cingolani, C., Palmer, P., 1996. The Argentine precordillera: a laurentian terrane? *GSA Today* 6, 16–18.
- DeMets, C., Gordon, R.G., Argus, D.F., 2010. Geologically current plate motions. *Geophysical Journal International* 181, 1–80.
- Figueroa, D.E., Ferraris, O.R., 1989. Estructura del Margen oriental de la Precordillera Mendocina-Sanjuanina. In: Primer Congreso Nacional de Exploración de Hidrocarburos. Mar del plata. Universidad de Buenos Aires, Buenos Aires.
- Finney, S.C., 2007. The parautochthonous Gondwanan origin of the Cuyania (greater Precordillera) terrane of Argentina: a re-evaluation of evidence used to support an allochthonous Laurentian origin. *Geologica Acta* 5, 127–158.
- Fromm, R., Zandt, G., Beck, S., 2004. Crustal thickness beneath the Andes and Sierras Pampeanas at 30°S inferred from Pn apparent phase velocities. *Geophysical Research Letters* 31, 1–4.
- Gans, C.R., Beck, S.L., Zandt, G., Gilbert, H., Alvarado, P., Anderson, M., Linkimer, L., 2011. Continental and oceanic crustal structure of the pampean flat slab region, western Argentina, using receiver function analysis: new high-resolution results. *Geophysical Journal International* 186, 45–58.
- Gilbert, H., Beck, S., Zandt, G., 2006. Lithospheric and upper mantle structure of central Chile and Argentina. *Geophysical Journal International* 165, 383–398.
- González Bonorino, G., 1973. Sedimentología de la Formación Punta Negra y algunas consideraciones sobre la geología regional de la precordillera de San Juan y Mendoza. *Revista de la Asociación Geológica Argentina* 30, 223–246.
- Gurrola, H., Minster, J.B., Owens, T., 1994. The use of velocity spectrum for stacking receiver functions and imaging upper mantle discontinuities. *Geophysical Journal International* 117, 427–440.
- Hayes, G., Furlong, K.P., 2007. Abrupt changes in crustal structure beneath the Coast Ranges of northern California developing new techniques in receiver function analysis. *Geophysical Journal International* 170, 313–336.
- Introcaso, A., Pacino, M.C., Fraga, H., 1992. Gravity, Isostasy and Andean crustal shortening between latitudes 30 and 35°S. *Tectonophysics* 205, 31–48.
- Isacks, B.L., Jordan, T., Allmendinger, R., Ramos, V.A., 1982. La segmentación tectónica de los Andes centrales y su relación con la placa de Nazca subductada. V Congreso Latinoamericano de Geología (Buenos Aires), Actas 3, 587–606.
- Jin, Z.-M., Zhang, J., Green, H.W., 2001. Eclogite rheology: implications for subducted lithosphere. *Geology* 29–8, 667–670.
- Jordan, T., Allmendinger, R., 1986. The Sierras pampeanas of Argentina: A modern analogue of Rocky Mountain foreland deformation. *American Journal of Science* 286, 737–764.
- Jordan, T., Isacks, B.L., Allmendinger, R., Brewer, J., Ramos, V., Ando, C.J., 1983. Andean Tectonics related to geometry of subducted Nazca plate. *Geological Society of America, Bulletin* 94 (3), 341–361.
- Kay, S., Abbruzzi, J., 1996. Magmatic evidence for Neogene lithospheric evolution of the Central Andean flat-slab between 30 and 32°S. *Tectonophysics* 259, 15–28.
- Langston, C.A., 1979. Structure under Mount Rainier, Washington, inferred from teleseismic body waves. *Journal of Geophysical Research* 84, 4749–4762.
- Ligorria, J., Ammon, C.J., 1999. Iterative deconvolution and receiver function estimation. *Bulletin of the Seismological Society of America* 89, 1395–1400.
- Linkimer, L., 2011. Lithospheric Structure of the Pampean Flat Slab (Latitude 30–33S) and Northern Costa Rica (Latitude 9–11N) Subduction Zones. Dissertation (Ph.D.). University of Arizona, Tucson, Arizona, United States of America.
- Linkimer, L., Beck, S.L., Schwartz, S.Y., Zandt, G., Levin, V., 2010. Nature of crustal terranes and the Moho in northern Costa Rica from receiver function analysis. *Geochemistry Geophysics Geosystems* 11, 1–24.
- Ludwig, W.J., Nafe, J.E., Drake, C.L., 1970. Seismic refraction. In: Maxwell, A.E. (Ed.), 1970. The Sea, vol. 4. Wiley-Interscience, New York, pp. 53–84.
- McGlashan, N., Brown, L., Kay, S., 2008. Crustal thickness in the central Andes from teleseismically recorded phase precursors. *Geophysical Journal International* 175, 1013–1022.
- Pakiser, L.C., Robinson, R., 1966. Composition and evolution of the continental crust as suggested by seismic observations. *Tectonophysics* 59, 547–557.
- Pardo, M., Comte, D., Monfret, T., 2002. Seismotectonics and stress distribution in the central Chile subduction zone. *Journal of South American Earth Sciences* 15, 11–22.
- Perarnau, M., Alvarado, P., Saez, M., 2010. Estimación de la estructura cortical de velocidades sísmicas en el suroeste de la Sierra de Pie de Palo, Provincia de San Juan. *Revista de la Asociación Geológica Argentina* 64, 473–480.
- Perarnau, M., Gilbert, H., Alvarado, P., Martino, R., Anderson, M., 2012. Crustal structure of the Eastern Sierras Pampeanas of Argentina using high frequency local receiver functions. *Tectonophysics* 580, 208–217.
- Pilger Jr., R.H., Handshumacher, D.W., 1981. The fixed-hotspot hypothesis and origin of the Easter-Sala y Gomez-Nazca trace. *Geological Society of America Bulletin* 92, 1437–1446.
- Ramos, V.A., 1988. The tectonics of the Central Andes: 30° to 33°S latitude. In: Clark, S.P., Clark Burchfiel, J.B., Suppe, J. (Eds.), Processes in Continental Lithospheric Deformation. Geological Society of America, Boulder, Colo, pp. 31–54.
- Ramos, V.A., 1995. Sudamérica: un mosaic de continentes y océanos. *Ciencias Hoy* 6, 24–29.
- Ramos, V.A., 2004. Cuyania, an exotic block to Gondwana: review of a historical success and the present problems. *Gondwana Research* 7 (4), 1009–1026.
- Ramos, V.A., 2009. Anatomy and global context of the Andes: main geologic features and the Andean orogenic cycle. *The Geological Society of America, Memoir* 204. Boulder, Colorado.
- Ramos, V.A., Kay, S.M., 1991. Triassic rifting and associated basalt in the Cuyo basin, Central Argentina. In: Harmon, R.S., Rapela, C.W. (Eds.), 1991. Andean Magmatism and Its Tectonic Setting, vol. 265. Geological Society of America, pp. 79–91.
- Ramos, V.A., Jordan, T.E., Allmendinger, R.W., Mpodozis, M.C., Kay, S.M., Cortes, J.M., Palma, M., 1986. Paleozoic terranes of the central Argentine-Chilean Andes. *Tectonics* 5, 855–880.
- Ramos, V.A., Dallmeyer, R.D., Vujovich, G.I., 1998. Time constraints on the early Paleozoic docking of the Precordillera, central Argentina. In: Pankhurst, R.J., Rapela, C.W. (Eds.), The Proto-Andean Margin of Gondwana, Geological Society Special Publications, vol. 142, pp. 143–158.
- Ramos, V.A., Cristallini, E.O., Pérez, D.J., 2002. The Pampean flat-slab of the central Andes. *Journal of South American Earth Sciences* 15, 59–78.
- Sato, A.M., Tickij, H., Llambías, E.J., Stipp Basei, M.A., González, P.D., 2004. Las Matras block, central Argentina (37°S–67°W): the southernmost Cuyania terrane and its relationship with the Famatinian orogeny. *Gondwana Research* 7 (4), 1077–1087.
- Scholz, C.H., 1990. The Mechanics of Earthquakes and Faulting. Cambridge University Press, Cambridge.

- Smalley, R., Pujol, J., Regnier, M., Chiu, J.-M., Chatelain, J.L., Isacks, B.L., Araujo, M., Puebla, N., 1993. Basement seismicity beneath the Andean precordillera, thin-skinned thrust belt and implications for crustal and lithospheric behavior. *Tectonics* 12, 63–76.
- Taylor, S.R., McLennan, S.M., 1981. The composition and evolution of the continental crust; rare earth element evidence from sedimentary rocks. *Philosophical Transactions of the Royal Society London A* 301, 381–399.
- Uliana, M.A., Arteaga, M.E., Legarreta, L., Cerdán, J.J., Peroni, G.O., 1995. Inversion structures and hydrocarbon occurrence in Argentina, in Basin inversion. In: Buchanan, J.G., Buchanan, P.G. (Eds.), 1995. Geological Society Special Publication, vol. 88, pp. 211–233.
- UNCUYO, 2012. Informe científico de la Universidad Nacional de Cuyo. <http://www.uncu.edu.ar/novedades/index/informe-cientifico-que-estudia-el-aconcagua-el-coloso-de-america-mide-69608-metros>.
- Vergés, J., Ramos, V.A., Meigs, A., Cristallini, E., Bettini, F.H., Cortés, J.M., 2007. Crustal wedging triggering recent deformation in the Andean thrust front between 31°S and 33°S: Sierras Pampeanas–Precordillera interaction. *Journal of Geophysical Research* 112, B03S15. <http://dx.doi.org/10.1029/2006JB004287>.
- Von Gosen, W., 1992. Structural evolución of the Argentine precordillera: the Rio San Juan section. *Journal of Structural Geology* 14, 643–667.
- Wagner, L.S., Anderson, M.L., Jackson, J.M., Beck, S.L., Zandt, G., 2008. Seismic evidence for orthopyroxene enrichment in the continental lithosphere. *Geology* 36, 935–938.
- Weaver, B.L., Tarney, J., 1984. In: Pollack, H.N., Murthy, V.R. (Eds.), Major and Trace Element Composition of the Continental Lithosphere. Pergamon, New York, United States of America, pp. 39–68.
- Yáñez, G., Cembrano, J., Pardo, M., Ranero, C., Selles, D., 2002. The Challenger-Juan Fernández-Maipo major tectonic transition of the Nazca-Andean subduction system at 33–34°S: geodynamic evidence and implications. *Journal of South American Earth Sciences* 15, 23–38.
- Zapata, T.R., 1998. Crustal structure of the Andean thrust front at 30°S latitude from shallow and deep seismic reflection profiles, Argentina. *Journal of South American Earth Sciences* 11, 131–151.